International Conference on Recent Advances in Fluid Mechanics and Nanoelectronics, MIT, Bengaluru

A numerical study on the influence of geometry on the rupture risk of abdominal aortic aneurysms

G R Krishna Chand Avatar, Chinika Dangi, Puneet Pushkar

Department of Aerospace Engineering

Indian Institute of Science, Bengaluru

July 13, 2023

Overview

Abdominal aortic aneurysms: A brief introduction

- Aneurysm: Local abnormal dilatation of an artery with respect to its original state due to weakening of its wall
- 80 % of aortic aneurysms are found in abdominal region and are called abdominal aortic aneurysms (AAAs)
- AAA defined as the portion of infrarenal segment with aortic diameter at least 1.5 times the normal diameter, that is, 2 cm[1]

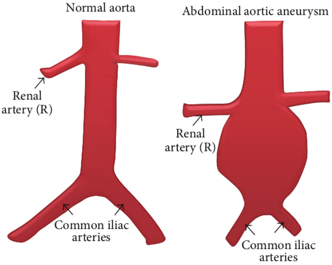

Source: Canchi et al.[2]

[1] Aggarwal et al., "Abdominal aortic aneurysm: A comprehensive review".

[2] Canchi et al., "A Review of Computational Methods to Predict the Risk of Rupture of Abdominal Aortic Aneurysms".

AAAs: Incidence rates and predispossessing factors

- No official statistics of incidence of AAAs in India; some studies suggest very low incidence in India[3].
- Several risk factors responsible for growth, genesis and rupture of AAAs, namely
  - People aged > 60 years
  - 6 times higher in males than females
  - Atherosclerosis (thrombus deposition), hypertension, smoking, coronary heart disease
- Asymptomatic until rupture, detected during diagnosis for unrelated causes.
- Surgeons use maximum transverse diameter of 5-5.5 cm for surgical repair as rupture risk criterion; not always the case.
- Better criterion should be based on hemodynamics, such as wall shear stress (WSS) and other derived quantities, and wall mechanics simulations (wall stress)[4].

[3] Unnikrishnan et al., "Aortic diseases in India and their management: An experience from two large centers in South India".

[4] Mutlu et al., "How does hemodynamics affect rupture tissue mechanics in abdominal aortic aneurysm: Focus on wall shear stress derived parameters, time-averaged wall shear stress, oscillatory shear index, endothelial cell activation potential, and relative residence time"; Raghavan and Vorp, "Toward a biomechanical tool to evaluate rupture potential of abdominal aortic aneurysm: identification of a finite strain constitutive model and evaluation of its applicability".

Literature review

- Bluestein et al.[5] concluded that fluid dynamics characterising flow recirculation region formed inside the aneurysm created suitable conditions encouraging thrombus formation and the viability of aneurysm rupture.
- Boyd et al.[6] observed that aortic rupture took place at the sites of reduced flow velocity, mostly, in recirculation flow regions, where low WSS and relatively more intraluminal thrombus deposition persisted but not at the site of maximum pressure and WSS.
- Philip et al.[7] postulated that high TAWSS and low OSI indicates the initiation of intraluminal thrombus (ILT) formation.
- Venkatasubramaniam et al.[8] did FE analysis on 27 patient-specific AAA geometries and found that peak wall stress for ruptured aneurysms is about 60% higher than for the nonruptured ones. They also discovered that the area of peak wall stress correlated with rupture site.

---

[5] Bluestein et al., "Steady Flow in an Aneurysm Model: Correlation Between Fluid Dynamics and Blood Platelet Deposition".

[6] Boyd et al., "Low wall shear stress predominates at sites of abdominal aortic aneurysm rupture".

[7] Philip, B. S. V. Patnaik, and J., "Fluid structure interaction study in model abdominal aortic aneurysms: Influence of shape and wall motion"; Philip, B. Patnaik, and Sudhir, "Hemodynamic simulation of abdominal aortic aneurysm on idealised models: Investigation of stress parameters during disease progression".

[8] Venkatasubramaniam et al., "A Comparative Study of Aortic Wall Stress Using Finite Element Analysis for Ruptured and Non-ruptured Abdominal Aortic Aneurysms".

Problem description

- Martufi et al.[9] extracted 3D patient-specific geometries from CT images of 9 patients with AAA and evaluated 1D geometric indices: D_{max}, D_{neck1}, D_{neck2}, H_b, H, L, d_c, d
- Six shape indices:
  $\mathrm{DHr} = \frac{D_{max}}{H}$, $\mathrm{DDr} = \frac{D_{max}}{D_{neck1}}$, $\mathrm{Hr} = \frac{H}{H_{neck}}$, $\mathrm{BL} = \frac{H_b}{H}$, $\beta = 1 - \frac{d_c}{D_{max}}$, $T = \frac{L}{d}$
- For idealised fusiform AAA geometries: $\beta = T = 1$

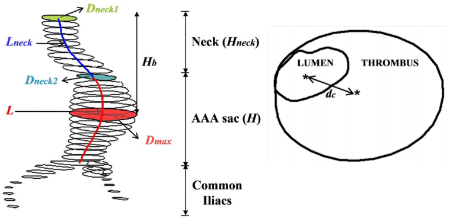

- We study effect of DHr using two AAA geometries, AAA1 and AAA2 (AAA2 has higher DHr)

	AAA1	AAA2
DHr	0.83	0.45
DDr	2	2
Hr	2.4	3.67
BL	0.92	0.77

[9] Martufi et al., "Three-Dimensional Geometrical Characterization of Abdominal Aortic Aneurysms: Image-Based Wall Thickness Distribution".

Fluid dynamics model of blood

- Blood is considered to be incompressible fluid in an isothermal flow regime.
- We use Newtonian and non-Newtonian Carreau-Yasuda models for blood.
- The governing equations in integral form are
  - Continuity equation for incompressible flows: $\int_S \rho^f \boldsymbol{v}^f \cdot \boldsymbol{n} dS = 0$
  - Momentum balance equation:

$$\frac{\partial}{\partial t}\int_V \rho^f \boldsymbol{v}^f(\boldsymbol{x},t)dV + \oint_S \rho^f \boldsymbol{v}^f(\boldsymbol{v}^f \cdot \boldsymbol{n})dS = \oint_S \boldsymbol{\sigma}^f \cdot \boldsymbol{n} dS \qquad (1)$$

    where ρ^f is fluid density, $\boldsymbol{v}^f$ is velocity of the flow field, $\boldsymbol{\sigma}^f$ is Cauchy stress tensor.
  - Constitutive relation for Newtonian fluid:
    $\boldsymbol{\sigma}^f = -p\boldsymbol{I} + \mu^f\left(\boldsymbol{\nabla}\boldsymbol{v}^f + (\boldsymbol{\nabla}\boldsymbol{v}^f)^T\right) - \frac{2}{3}\mu^f(\boldsymbol{\nabla}\cdot\boldsymbol{v}^f)\boldsymbol{I}$ where p is pressure field.
  - Material parameters[10]: Density, $\rho^f = 1050$ kg/m^3 and transport properties are
    - Newtonian model: dynamic viscosity $\mu^f = 0.0044$ Pa-s
    - Carreau-Yasuda model: dynamic viscosity $\mu^f = \mu_\infty + (\mu_0 - \mu_\infty)[1 + (\lambda\dot{\gamma})^a]^{(n-1)/a}$ where $\mu_0 = 0.16$ Pa-s, $\mu_\infty = 0.0035$ Pa-s, $\lambda = 8.2$ s, $n = 0.2128$, $a = 0.64$ and shear rate, $\dot{\gamma}$ is calculated as

$$\dot{\gamma} = \sqrt{2\,\mathrm{tr}(\boldsymbol{D}:\boldsymbol{D})} \quad ; \boldsymbol{D} = \left(\frac{\boldsymbol{\nabla}\boldsymbol{v} + (\boldsymbol{\nabla}\boldsymbol{v})^T}{2}\right)$$

[10] Biasetti, Hussain, and Gasser, "Blood flow and coherent vortices in the normal and aneurysmatic aortas: a fluid dynamical approach to intra-luminal thrombus formation".

Fluid dynamics model of blood: Boundary conditions

- Inlet: Time-varying paraboloid velocity profile is imposed $v_z(r,t) = 2v_{z,avg}(t)\left(1-\left(\frac{r}{R}\right)^2\right)$. Here, an 8-series Fourier decomposition of cross-sectional average value is obtained using MATLAB® as

$$v_{z,avg}(t) = a_0^{\boldsymbol{v}} + \sum_{k=1}^{8}\left[a_k^{\boldsymbol{v}}\cos\left(k\omega t\right) + b_k^{\boldsymbol{v}}\sin\left(k\omega t\right)\right]$$

  where $\omega = \frac{2\pi k}{T}$, $T = 1$ s is time-period of cardiac cycle, $a_0^{\boldsymbol{v}}, a_i^{\boldsymbol{v}}, b_i^{\boldsymbol{v}}$ $(i \in \{1, 2, \cdots, 8\})$ are the corresponding Fourier components. Zero-gradient condition is used for pressure.
- Outflow boundaries: Uniform time-varying pressure in terms of an 8-series Fourier decomposition is used, $p(t) = a_0^p + \sum_{k=1}^{8}\left[a_i^p\cos\left(k\omega t\right) + b_k^p\sin\left(k\omega t\right)\right]$. Zero-gradient condition is used for velocity.
- Endoluminal surface of AAA wall: No-slip condition for velocity, $\boldsymbol{v} = \boldsymbol{0}$ and zero-gradient for pressure field.

Fluid dynamics model of blood: Boundary conditions

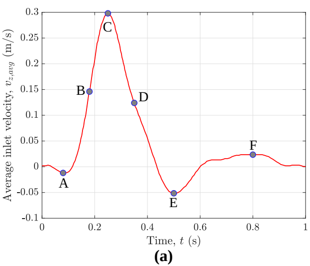

Waveforms for (a) Average inlet velocity with markers indicating time instants: initiation of systole A (t = 0.08 s), systolic acceleration B (t = 0.18 s), peak systole C (t = 0.25 s), systolic deceleration D (t = 0.35 s), beginning of diastole E (t = 0.50 s), late diastole F (t = 0.80 s) (b) Outlet pressure with marker A (t = 0.32 s) indicating peak pressure.[11]

[11] Philip, B. S. V. Patnaik, and J., "Fluid structure interaction study in model abdominal aortic aneurysms: Influence of shape and wall motion".

Solid dynamics model of AAA wall

- AAA wall is considered to be isotropic, homogeneous, compressible.
- Constitutive modeling of AAA wall has been performed using linear elastic and non-linear elastic models (Saint Venant Kirchhoff and Raghavan-Vorp elastic[12]).
- Mechanical properties of AAA wall: density $\rho^s = 2000$ kg/m^3, material constants are
  - Linear and Saint Venant Kirchhoff elastic models: $E = 2.7 \times 10^6$ Pa, $\nu^s = 0.45$
  - Raghavan-Vorp model: $\alpha = 1.74 \times 10^5$ Pa, $\beta = 1.881 \times 10^6$ Pa, $\nu^s = 0.45$

  The wall thickness is considered to be uniform with a value of 1.2 mm[13].
- Deformation gradient tensor, $\boldsymbol{F} = \boldsymbol{I} + \boldsymbol{\nabla}_0 \boldsymbol{u}$ where $\boldsymbol{u}$ is displacement and subscript 0 indicates differentiation with respect to initial configuration.
- Balance of linear momentum for a deformable solid is mathematically expressed as

$$\rho_0^s \frac{\partial^2 \boldsymbol{u}}{\partial t^2} = \boldsymbol{\nabla}_0 \cdot \boldsymbol{P} \qquad \text{where } \boldsymbol{P} \text{ is first Piola-Kirchhoff (PK) stress tensor}$$

- Relation between $\boldsymbol{P}$ and $\boldsymbol{S}$ (2^{nd} PK tensor), and Cauchy stress tensor $\boldsymbol{\sigma}^s$:
  $\boldsymbol{P} = \boldsymbol{F} \cdot \boldsymbol{S}, \qquad \boldsymbol{\sigma}^s = \frac{1}{J}\boldsymbol{P} \cdot \boldsymbol{F}^T = \frac{1}{J}\boldsymbol{F} \cdot \boldsymbol{S} \cdot \boldsymbol{F}^T \qquad (J = \det\{\boldsymbol{F}\})$

[12] Raghavan and Vorp, "Toward a biomechanical tool to evaluate rupture potential of abdominal aortic aneurysm: identification of a finite strain constitutive model and evaluation of its applicability".

[13] Philip, B. S. V. Patnaik, and J., "Fluid structure interaction study in model abdominal aortic aneurysms: Influence of shape and wall motion".

Solid dynamics model of AAA wall: Mathematical model

- Green-Lagrange strain tensor,

$$\boldsymbol{E} = \frac{1}{2}\left(\boldsymbol{F}^T \cdot \boldsymbol{F} - \boldsymbol{I}\right) = \underbrace{\frac{1}{2}\left(\boldsymbol{\nabla}_0 \boldsymbol{u} + (\boldsymbol{\nabla}_0 \boldsymbol{u})^T\right.}_{\text{linear part}} + \left.\underbrace{(\boldsymbol{\nabla}_0 \boldsymbol{u})^T \cdot \boldsymbol{\nabla}_0 \boldsymbol{u}}_{\text{non-linear part}}\right)$$

- **Linear elastic model** (isotropic Hooke's law): Captures small strains and small rotations

$$\boldsymbol{\sigma}^s = \boldsymbol{S} = 2\mu^s \boldsymbol{\epsilon} + \lambda^s \operatorname{tr}(\boldsymbol{\epsilon})\boldsymbol{I}, \qquad \boldsymbol{\epsilon} \text{ is linear part of } \boldsymbol{E}$$

- **Saint Venant Kirchhoff elastic model**: A non-linear model which captures small strains and finite rotations in an isotropic material

$$\boldsymbol{S} = 2\mu^s \boldsymbol{E} + \lambda^s \operatorname{tr}(\boldsymbol{E})\mathbf{I}$$

where $\mu^s = \frac{E}{2(1+\nu^s)}$ and $\lambda^s = \frac{\nu^s E}{(1+\nu^s)(1-2\nu^s)}$ are Lamé constants with Young's modulus E and Poisson's ratio ν^s.

- **Raghavan-Vorp elastic model**:

$$\boldsymbol{\sigma}^s = \frac{\kappa}{2}\left(J - \frac{1}{J}\right)\boldsymbol{I} + \operatorname{dev}\left(\frac{2}{J}\left[\alpha + 2\beta(I_{\overline{\boldsymbol{b}}} - 3)\right]\overline{\boldsymbol{b}}\right)$$

where $\overline{\boldsymbol{b}} = J^{-2/3}\boldsymbol{b}$ ($\boldsymbol{b} = \boldsymbol{F}\boldsymbol{F}^T$) and $\kappa = \frac{2}{3}\mu^s + \lambda^s$, $\mu^s = 2\alpha$

We have

$$\boldsymbol{\sigma}^s = \frac{1}{J}\boldsymbol{P} \cdot \boldsymbol{F}^T \qquad \Longrightarrow \quad \boldsymbol{P} = J\boldsymbol{\sigma}^s \boldsymbol{F}^{-T}$$

AEROSERVOELASTICITY LABORATORY

Solid dynamics model of AAA wall: Boundary conditions

- Side faces: zero displacement, that is, $\boldsymbol{u} = \mathbf{0}$, is imposed.
- Internal (endoluminal) surface: For solid dynamics simulations, a time-varying uniform pressure loading p corresponding to cardiac cycle is used such that traction is

$$\boldsymbol{t}^s = -p\boldsymbol{n}^s$$

- External surface: Traction-free Neumann boundary condition, $\boldsymbol{t}^s = \boldsymbol{\sigma}^s \cdot \boldsymbol{n}^s = \mathbf{0}$ is used.

Numerical discretization of mathematical models

- **Fluid**: Pressure Implicit with Splitting of Operators (PISO) algorithm[14] is used to solve the discretised system of equations in a segregated fashion. An unconditionally stable second-order accurate backward Euler scheme is used to advance the simulation.
- **Solid**: Second-order accurate backward Euler scheme is used for time integration.
- An open-source software package called *solids4Foam* alongwith *foam-extend 4.0*[15], a branch of the widely known software for CFD simulations called OpenFOAM, is used.

AEROSERVOELASTICITY LABORATORY

[14] Moukalled, Mangani, and Darwish, *The Finite Volume Method in Computational Fluid Dynamics*.
[15] Jasak et al., *foam-extend 4.0: Open Source CFD Toolbox*.

Geometry and mesh generation

- AAA lumen geometry in terms of the maximum diameter D_{max}, proximal neck diameter D_{neck2} and height of the sac H is expressed as

$$r(z) = \left(\frac{D_{max} - D_{neck2}}{4}\right)\left[1 + \sin\left(\frac{2\pi z}{H} - \frac{\pi}{2}\right)\right] + \frac{D_{neck2}}{2} \quad ; \quad 0 \leq z \leq H$$

  We consider $D_{neck1} = D_{neck2}$ and $D_{max} = 5$ cm[16]

- For proper imposition of BCs, the inlet and outlet extensions should be greater than or equal to[17] $\int_0^T v_{z,avg} dt \approx 5 \times 10^{-2}$ m which is twice the proximal neck diameter $2D_{neck2}$.

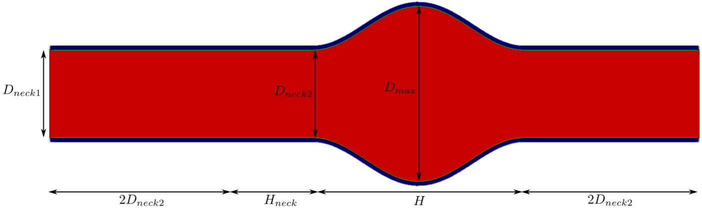

[16] Philip, B. S. V. Patnaik, and J., "Fluid structure interaction study in model abdominal aortic aneurysms: Influence of shape and wall motion".

[17] Krishna et al., "Shear stress rosettes capture the complex flow physics in diseased arteries".

Geometry and mesh generation

- AAA lumen geometries generated using an open-source CAD software *Salome*
- An open-soure OpenFOAM-based mesh generation tool called *cfMesh*[18] was used to generate fluid mesh for AAA lumen comprising of predominantly hexahedral cells.
- Solid mesh for each AAA geometry was generated by extruding the wall patch of the fluid mesh using *extrudeMesh*.

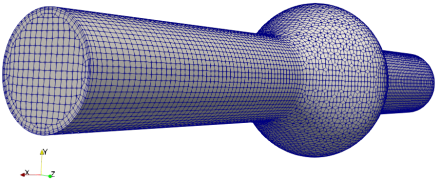

Fluid mesh

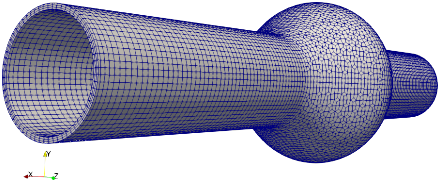

Solid mesh

[18] Juretic and Baburic, *cfMesh: A library for polyhedral mesh generation.*

Hemodynamic and arterial wall stress parameters

- Wall shear stress (WSS) and other derived quantities[19]:
  WSS vector, $\boldsymbol{\tau}_w$: Tangential part of traction vector $\boldsymbol{t}$; $\boldsymbol{t} = \boldsymbol{\sigma}^f \cdot \boldsymbol{n}^f$, where $\boldsymbol{\sigma}^f$ is Cauchy stress tensor and $\boldsymbol{n}^f$ is wall normal unit vector.

$$\boldsymbol{\tau}_w = \boldsymbol{t} - (\boldsymbol{t} \cdot \boldsymbol{n}^f)\boldsymbol{n}^f$$

  - Mean wall shear stress, $meanWSS(\boldsymbol{x}) = \left\| \frac{1}{T} \int_0^T \boldsymbol{\tau}_w(\boldsymbol{x}, t) dt \right\|$
  - Time-averaged wall shear stress, $TAWSS(\boldsymbol{x}) = \frac{1}{T} \int_0^T \|\boldsymbol{\tau}_w(\boldsymbol{x}, t)\| dt$
  - Oscillatory shear index (OSI): Characterises whether WSS vector is aligned with $TAWSS$ vector throughout cardiac cycle,

$$OSI(\boldsymbol{x}) = \frac{1}{2}\left(1 - \frac{meanWSS(\boldsymbol{x})}{TAWSS(\boldsymbol{x})}\right)$$

    OSI varies from 0 to 0.5.
- Arterial wall stress:
  - von Mises stress σ_{eq} is defined as

$$\sigma_{eq} = \frac{1}{\sqrt{2}} \sqrt{(\sigma_{xx} - \sigma_{yy})^2 + (\sigma_{yy} - \sigma_{zz})^2 + (\sigma_{xx} - \sigma_{zz})^2 + 6(\sigma_{xy}^2 + \sigma_{yz}^2 + \sigma_{xz}^2)}$$

    where σ_{ij} $(i, j = x, y, z)$ are the components of Cauchy stress tensor $\boldsymbol{\sigma}^s$.
  - Maximum principal stress σ_1 is the maximum eigenvalue of $\boldsymbol{\sigma}^s$.

[19] Oliveira et al., "A longitudinal study of a lateral intracranial aneurysm: identifying the hemodynamic parameters behind its inception and growth using computational fluid dynamics".

AEROSERVOELASTICITY LABORATORY

Hemodynamics simulations in AAA lumen geometries

- Hemodynamics simulations are performed using Newtonian and Carreau-Yasuda constitutive models for blood; AAA walls are assumed to be rigid.
- Numerical simulations done for 4 cardiac cycles to achieve solution periodicity in time.
- Simulation details for mesh sensitivity of AAA1 lumen:

	Coarse	Medium	Fine
Number of cells (in millions)	1.82	3.66	6.8
Number of prismatic layers at the wall	5	9	12
Time-step size (in seconds)	2×10^{-4}	1×10^{-4}	5×10^{-5}

- Time-step sizes chosen such that maximum Courant-Friedrichs-Levy (CFL) number (CFL ≤ 1) throughout every simulation (although an unconditionally stable implicit time-integration scheme is used).

Effect of blood constitutive models: Vortex dynamics

- Vortex dynamics of AAA1: (a) Vorticity contours and λ_2 iso-surface for Carreau-Yasuda model, (b) $\lambda_2 = -75\ \mathrm{s}^{-1}$ iso-surface for Newtonian model.

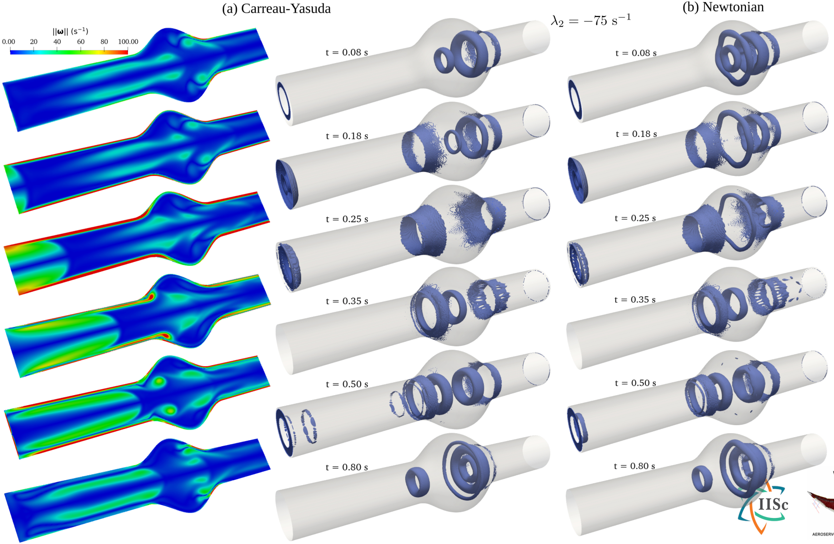

Effect of blood constitutive models: $TAWSS$ and OSI distribution

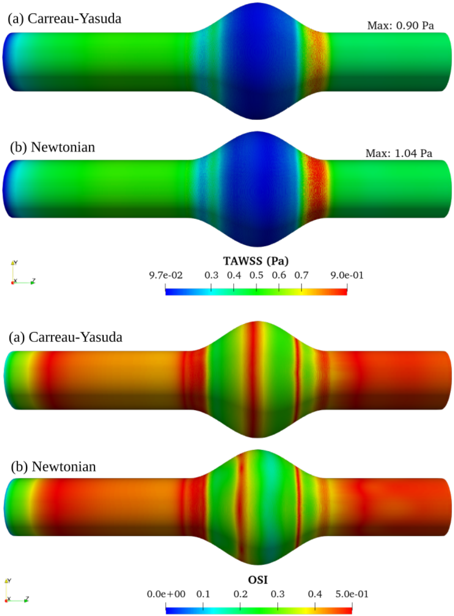

Effect of DHr: Vortex dynamics

- Vortex dynamics: $\lambda_2 = -75\ \mathrm{s}^{-1}$ iso-surface contours for (a) AAA1 (b) AAA2.

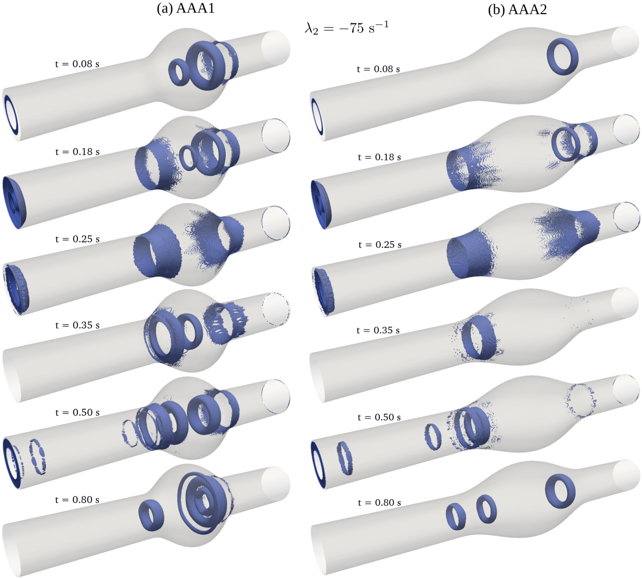

Effect of DHr: $TAWSS$ and OSI distribution for (a) AAA1 (b) AAA2

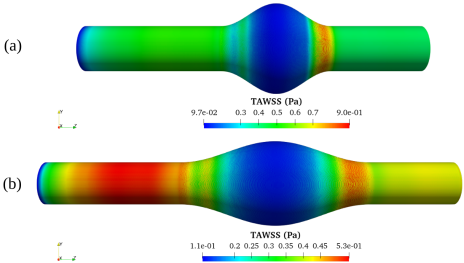

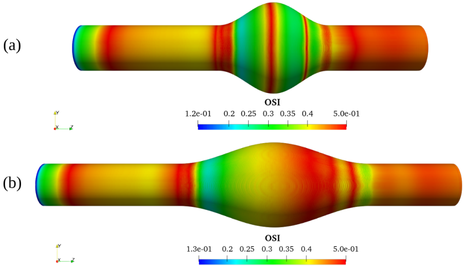

AAA wall mechanics simulations

- Endoluminal (inner) surface of AAA1 and AAA2 walls subjected to time-varying uniform pressure loading corresponding to the cardiac cycle.
- Mesh information for mesh sensitivity analysis of AAA1 wall:

	No of cells in radial direction	No of cells
Coarse	3	31,500
Medium	5	73,800
Fine	8	1,63,700

- Time step chosen for mesh sensitivity: 5×10^{-3} s
- For temporal sensitivity analysis, medium mesh is chosen.

Effect of solid constitutive models for AAA1 wall

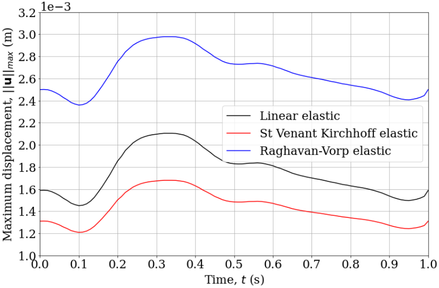

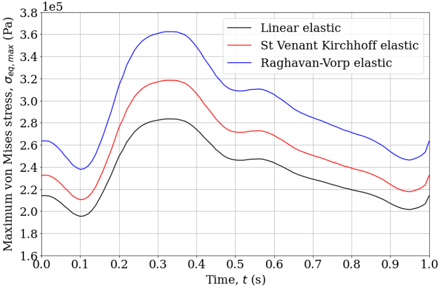

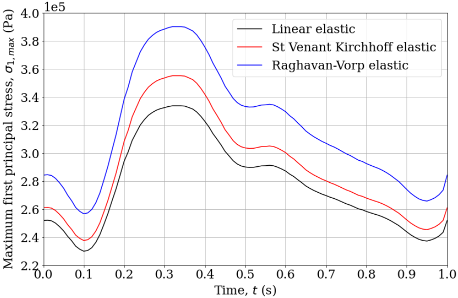

AAA wall mechanics simulations: AAA1 versus AAA2 walls

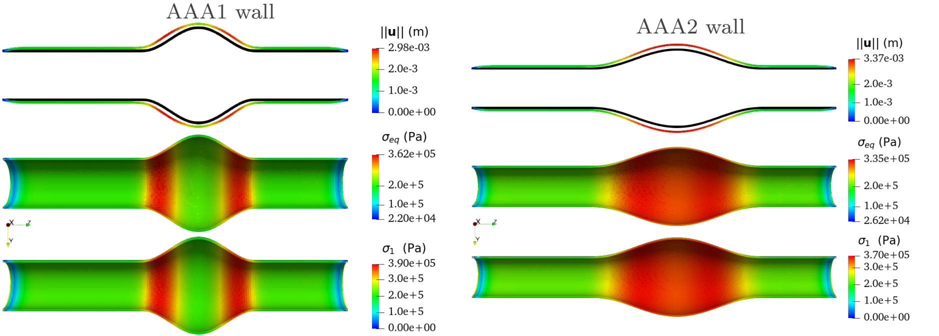

- Total displacement (top), von Mises stress (middle), first principal stress (bottom) for AAA walls modeled as Raghavan-Vorp elastic material under peak uniform pressure loading at $t = 0.32$ s

Effect of DHr: AAA1 versus AAA2

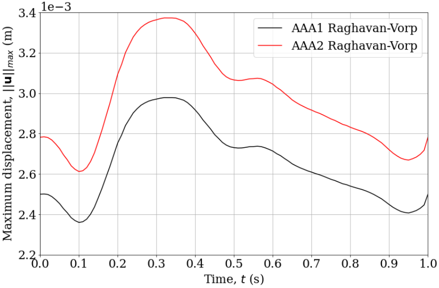

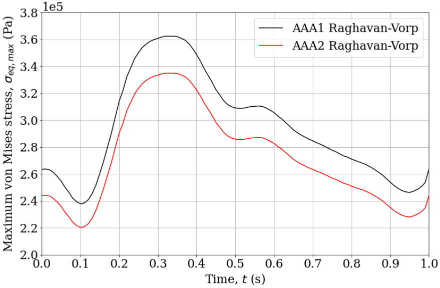

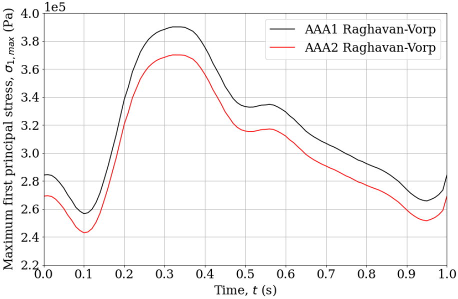

Conclusion

- Influence of shape index DHr, ratio of maximum transverse diameter to abdominal height, is investigated using two AAA geometries, AAA1 with higher DHr than AAA2.

- Hemodynamics inside AAAs:
  - Effect of Newtonian and Carreau-Yasuda constitutive models: The vortex dynamics and recirculation patterns are quite similar in both cases. $TAWSS$ values are higher in Newtonian case.
  - Effect of DHr: Recirculation regions persist for longer time in AAA1 than in AAA2. Vortex dynamics in AAA1 is more proactive. Maximum $TAWSS$ are higher in AAA1.
  - AAA1 (AAA with higher DHr) is susceptible to increased thrombus deposition and thus a higher probability of rupture than AAA2.

- AAA wall mechanics simulations:
  - Effect of constitutive models: Linear elastic and Saint Venant Kirchhoff elastic models underpredict maximum displacement, maximum von Mises stress, maximum first principal stress compared to Raghavan-Vorp elastic model.
  - Effect of DHr: For the case of Raghavan-Vorp elastic model, both maximum von Mises and maximum first principal stresses are found to be higher for AAA1 wall while the maximum displacement of AAA1 wall is lower than that of the AAA2.
  - AAA1 is at a higher risk of rupture than AAA2.

References I

- Aggarwal, Sourabh et al. "Abdominal aortic aneurysm: A comprehensive review". In: *Experimental and clinical cardiology* 16.1 (2011), pp. 11–15. URL: https://www.ncbi.nlm.nih.gov/pmc/articles/pmid/21523201/.
- Biasetti, Jacopo, Fazle Hussain, and T. Christian Gasser. "Blood flow and coherent vortices in the normal and aneurysmatic aortas: a fluid dynamical approach to intra-luminal thrombus formation". In: *Journal of The Royal Society Interface* 8.63 (Apr. 2011), pp. 1449–1461. DOI: 10.1098/rsif.2011.0041.
- Bluestein, D. et al. "Steady Flow in an Aneurysm Model: Correlation Between Fluid Dynamics and Blood Platelet Deposition". In: *Journal of Biomechanical Engineering* 118.3 (Aug. 1996), pp. 280–286. DOI: 10.1115/1.2796008.
- Boyd, April J. et al. "Low wall shear stress predominates at sites of abdominal aortic aneurysm rupture". In: *Journal of Vascular Surgery* 63.6 (June 2016), pp. 1613–1619. DOI: 10.1016/j.jvs.2015.01.040.
- Canchi, Tejas et al. "A Review of Computational Methods to Predict the Risk of Rupture of Abdominal Aortic Aneurysms". In: *BioMed Research International* 2015 (2015), pp. 1–12. DOI: 10.1155/2015/861627.
- Jasak, Hrvoje et al. *foam-extend 4.0: Open Source CFD Toolbox*. https://sourceforge.net/projects/foam-extend/. Accessed on 2021-04-06. Dec. 2016.
- Juretic, Franjo and Mario Baburic. *cfMesh: A library for polyhedral mesh generation*. https://cfmesh.com/cfmesh/. Accessed on 2021-06-11. July 2014.

References II

- Krishna, C. Vamsi et al. "Shear stress rosettes capture the complex flow physics in diseased arteries". In: *Journal of Biomechanics* 104 (May 2020), p. 109721. DOI: 10.1016/j.jbiomech.2020.109721.
- Martufi, Giampaolo et al. "Three-Dimensional Geometrical Characterization of Abdominal Aortic Aneurysms: Image-Based Wall Thickness Distribution". In: *Journal of Biomechanical Engineering* 131.6 (May 2009). DOI: 10.1115/1.3127256.
- Moukalled, F., L. Mangani, and M. Darwish. *The Finite Volume Method in Computational Fluid Dynamics*. Springer International Publishing, 2016. DOI: 10.1007/978-3-319-16874-6.
- Mutlu, Onur et al. "How does hemodynamics affect rupture tissue mechanics in abdominal aortic aneurysm: Focus on wall shear stress derived parameters, time-averaged wall shear stress, oscillatory shear index, endothelial cell activation potential, and relative residence time". In: *Computers in Biology and Medicine* 154 (Mar. 2023), p. 106609. DOI: 10.1016/j.compbiomed.2023.106609.
- Oliveira, I. L. et al. "A longitudinal study of a lateral intracranial aneurysm: identifying the hemodynamic parameters behind its inception and growth using computational fluid dynamics". In: *Journal of the Brazilian Society of Mechanical Sciences and Engineering* 43.3 (Feb. 2021). DOI: 10.1007/s40430-021-02836-6.

References III

Philip, Nimmy Thankom, B. S. V. Patnaik, and Sudhir B. J. “Fluid structure interaction study in model abdominal aortic aneurysms: Influence of shape and wall motion”. In: *International Journal for Numerical Methods in Biomedical Engineering* (Dec. 2020). DOI: 10.1002/cnm.3426.

Philip, Nimmy Thankom, B.S.V. Patnaik, and B.J. Sudhir. “Hemodynamic simulation of abdominal aortic aneurysm on idealised models: Investigation of stress parameters during disease progression”. In: *Computer Methods and Programs in Biomedicine* 213 (2022), p. 106508. DOI: 10.1016/j.cmpb.2021.106508. URL: https://doi.org/10.1016/j.cmpb.2021.106508.

Raghavan, M.L. and David A. Vorp. “Toward a biomechanical tool to evaluate rupture potential of abdominal aortic aneurysm: identification of a finite strain constitutive model and evaluation of its applicability”. In: *Journal of Biomechanics* 33.4 (Apr. 2000), pp. 475–482. DOI: 10.1016/s0021-9290(99)00201-8.

Unnikrishnan, Madathipat. et al. “Aortic diseases in India and their management: An experience from two large centers in South India”. In: *Indian Journal of Vascular and Endovascular Surgery* 3.1 (2016), pp. 20–23. DOI: 10.4103/0972-0820.180208.

Venkatasubramaniam, A.K et al. “A Comparative Study of Aortic Wall Stress Using Finite Element Analysis for Ruptured and Non-ruptured Abdominal Aortic Aneurysms”. In: *European Journal of Vascular and Endovascular Surgery* 28.2 (Aug. 2004), pp. 168–176. DOI: 10.1016/j.ejvs.2004.03.029.